Low temperature growth of superconducting Ta and Nb thin films for qubit application

Manisha Parthasarathy
2023 Physics REU, Department of Physics, University of California, Santa Barbara, Santa Barbara, CA 93106, USA and Department of Physics and Astronomy, Rutgers University, New Brunswick, New Jersey 08901, USA

Faculty Advisor: Christopher Palmstrøm
Department of Materials and Department of Electrical and Computer Engineering, University of California, Santa Barbara, Santa Barbara, CA 93106, USA

Graduate Advisor: Teun van Schijndel
Department of Electrical and Computer Engineering, University of California, Santa Barbara, Santa Barbara, CA 93106, USA
(Dated: October 5, 2023)

In the fields of superconducting and topological quantum computing, qubits are fabricated using high quality superconducting thin films. In general, thin films with poor electrical quality lead to a decrease in the critical temperature, making the critical temperature a good metric for the electrical quality of superconducting thin films. In this work, we explore methods of cryogenic molecular beam epitaxy (MBE) growth to increase the critical temperatures of superconducting Ta and Nb thin films on sapphire substrates. We compare the critical temperatures, critical magnetic fields, and residual resistance ratios of thin films grown at low temperature (cryostat cold head temperature <10 K) to those grown at room temperature and also investigate the effect of film thickness and substrates. We found that cryogenic MBE growth does result in higher critical temperatures compared to room temperature growth, most significantly for Ta thin films. Our measurements also indicated that the out-of-plane critical magnetic field does not change appreciably under low temperature growth of Nb thin films, although the width of the superconducting transition increases. When decreasing the sample thickness, we observed lower critical temperatures as expected, but higher critical magnetic field values, contrary to what we predicted. For low temperature growth on different substrates, we did not see any significant difference in critical temperature and magnetic field values. Structural analysis using X-ray diffraction shows that low temperature growth of Ta films results in the pure α-phase instead of a mixture of α and β phases.

I. INTRODUCTION

For two decades, creating multiqubit processors that have long coherence times has been the goal for superconducting quantum computation hardware realization [1]. Since these devices utilize quantum integrated circuits that must have low amounts of power dissipation and noise, superconducting circuit elements are especially useful in quantum bits (qubits) [2]. In particular, superconducting qubits use the nonlinear and dissipationless nature of Josephson tunnel junctions to establish a quantum two-level system with an anharmonic potential [1]. This allows us to store information in the unique energy differences between states, as shown in Figure 1[1]. Recently, qubits with coherence times approaching 0.5 milliseconds have been achieved, requiring great advancements in the field [3].

Additionally, recent advancements in topological quantum computation predict that gated 2D superconductor-semiconductor gate nanowire devices can host Majorana zero modes, which are useful for fault-tolerant qubits, shown in Figure 2[4, 5].

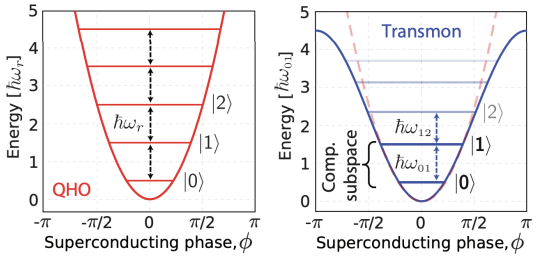

FIG. 1: Josephson junctions, made up of thin film superconductors, introduce anharmonicity to the potential of a system, allowing for information storage in the unique potential differences between states. [1]

By harnessing the properties of superconductors, the quality of qubits can be greatly improved and major advancements in superconducting and topo-

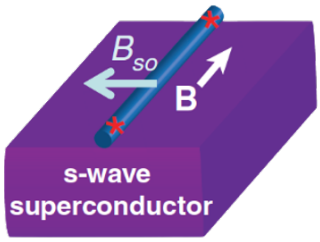

FIG. 2: The 2D superconductor-semiconductor nanowire device schematic for a topological qubit. [4]

logical quantum computation can be made. Both types of qubits require the use of thin film superconductors.

Common superconducting metals used include aluminum (Al), tantalum (Ta), and niobium (Nb) [3]. In order for a metal to enter the superconducting state, it must be in a regime below a certain critical temperature, T_C, depending on the metal. Typical T_C values for elemental superconductors range from 0 K to 10 K. According to the Meissner effect, the magnetic field inside a superconductor is always zero; however, there exists a critical magnetic field, H_C, dependent on the temperature of the system, above which the superconducting state of the metal will be broken. It is known that poor quality superconducting thin films lead to a decrease in T_C, affecting the suitability for use in qubit systems [6].

To combat this, we are interested in exploring methods of growth that increase the T_C value of our superconductors, in particular, refractory metals such as Ta and Nb. Previous studies have suggested that Ta films must be grown at high temperatures ($\sim$ 500 ℃) on sapphire or silicon (Si) substrates in order to achieve α-Ta, the phase of Ta with a body-centered cubic (BCC) lattice, as opposed to β-Ta, with a tetragonal structure. This results in critical temperatures of around 4 K, as opposed to less than 1 K [7, 8]. However, using Si substrates, high temperature growth causes the formation of tantalum-silicides on the superconductor-substrate interface, leading to dielectric loss [8]. Since dielectric loss from substrates affects qubit performance and coherence times, it is worth exploring methods of superconductor growth that avoid high temperatures [9]. High temperature growth also limits the use of other substrates and qubit materials; for example, InAs and InSb nanowires cannot be used in topological qubits when Ta and Nb thin films are grown at high temperatures, since they will decompose. This furthers our motivation to explore superconductor growth at lower temperatures. One study showed that by adding a Nb buffer layer between the Ta film and the substrate, α-Ta films without silicides can be grown at room temperature [8]. We seek alternative ways to grow our films on different substrates such that we observe the superconducting transition at higher T_C values. In this study, we use T_C as a metric for the electrical quality of thin films.

In this work, we explore low temperature superconducting thin film growth using a molecular beam epitaxy (MBE) system. We compare the T_C of samples grown at low temperature (cold head temperature <10 K) and room temperature (300 K), and investigate whether growth temperature affects film quality. Since topological qubits rely on the presence of a magnetic field, we investigate the effect of cryogenic film growth on the out-of-plane critical magnetic field values, as well [5]. In addition, as the thickness of the film decreases, the critical in-plane magnetic field increases; so, it is favorable to minimize the thickness of our superconducting films [4]. For this reason, we explore the T_C of samples with different film thickness under LT growth [10].

II. EXPERIMENT

We grew samples of Ta and Nb on Al_2O_3 substrates at low temperature and room temperature. The substrates were prepared with a 3-inch Al_2O_3(0001) wafer, which was coated and diced into 10x10 mm squares. We performed a solvent clean followed by a Piranha Etch (H_2SO_4:H_2O_2 3:1). Then, we annealed the surface in air at $\sim$ 1100 ℃ for 16 hours, and performed another Piranha etch. Finally, we did an in-situ ultra-high vacuum (UHV) anneal at $\sim$ 700 ℃. We then placed the substrate in a low temperature molecular beam epitaxy (LTMBE) system.

A. Low Temperature Molecular Beam Epitaxy

Our LTMBE system is a Scienta Omicron LT EVO 50 MBE chamber. The substrate was loaded in a UHV growth chamber with a base pressure of 2×10^{-11} mbar. For low temperature growth, the substrate was cooled on a 4 K cold head in the growth chamber. To evaporate the source material of Ta and Nb, the system utilized an electron beam source in a separate evaporation chamber, which is attached to the growth chamber. A gate valve be-

tween the chambers, when open, allows for deposition of the sample onto the substrate. The thickness of our films was measured using a quartz crystal monitor (QCM). With this setup, we grew samples of Ta, and Nb on Al_2O_3 with a nominal thickness of 50 nm at both room temperature and low temperature. Using a Si dioide mounted on the cold head, low temperature growth of Ta samples was measured to be at at 6.5 K and Nb at 5.5 K. We estimate that the sample temperature is, at maximum, about 10 K warmer. Lastly, we used atomic force microscopy (AFM) and X-ray diffraction (XRD) to analyze the surface morphology and crystal structures of our thin films.

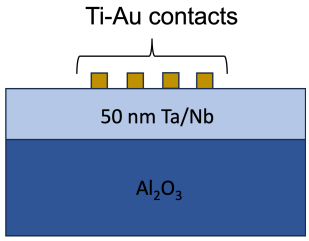

FIG. 3: Schematic of the final sample after adding Ti-Au contacts.

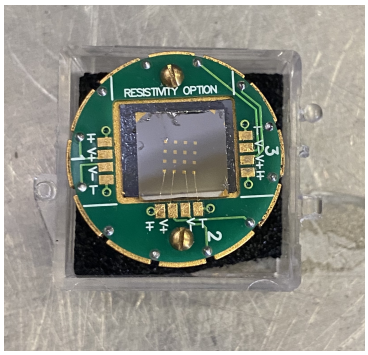

FIG. 4: Image of a sample on the Quantum Design resistivity puck, with four Au wires bonded for four-probe resistance measurements.

B. Physical Property Measurement System

To measure the resistance of our samples, we used a Quantum Design Physical Property Measurement System (PPMS). The PPMS contains a liquid helium cryostat which reaches temperatures as low as 2 K, and a superconducting magnet which generates fields up to 14 T.

After sample growth, we used shadow mask deposition and electron beam evaporation to make 4x4 Ti-Au contacts on the surface.

With a wire-bonding machine, we made four connections between the sample and a Quantum Design resistivity puck using gold wire for four probe resistance measurements, allowing us to minimize the effect of contact resistance. In the PPMS, we applied a current of 100 μA between two contacts on the puck and measured the voltage difference between the other two contacts. The resistance was calculated while performing temperature sweeps between 2 K and 300 K. For critical field measurements, we also performed out-of-plane magnetic field sweeps at constant temperatures below the observed critical temperature.

III. RESULTS AND DISCUSSION

A. Critical Temperature Comparison

For each sample, we plotted the resistivity against the temperature to find the superconducting transition, shown in Figure 5. To calculate resistivity, we used the resistance measurements from the PPMS and computed

$$\rho = R \cdot \pi \cdot d / \ln(2) \tag{1}$$

where R is the measured resistance and d is the thickness of the sample. To approximate the value of T_C, we found the temperature at which the resistance was 50% of the maximum resistance for temperatures from 2 K to 10 K. We also calculated the residual resistance ratio (RRR), where we define:

$$RRR = R_{300K}/R_{10K} \tag{2}$$

Since higher RRR values are associated with longer relaxation times in qubits, we use it as another metric for thin film quality [11].

From this data, we observe that the T_C for 50 nm of Ta grown at RT must be < 2 K, since no superconducting transition was seen. However, for LT growth, the superconducting transition was seen around 4.15 K. We also saw an increase in the RRR, from 1.04 under RT growth, to 16.9 under LT growth. This means that as the RT grown samples were cooled down from 300 K to 2 K, the resistivity stayed about the same, whereas the resistivity for the LT grown samples decreased dramatically. This evidence suggests that LT MBE growth results in higher quality Ta thin films.

For Nb, we also saw an increase in the T_C and

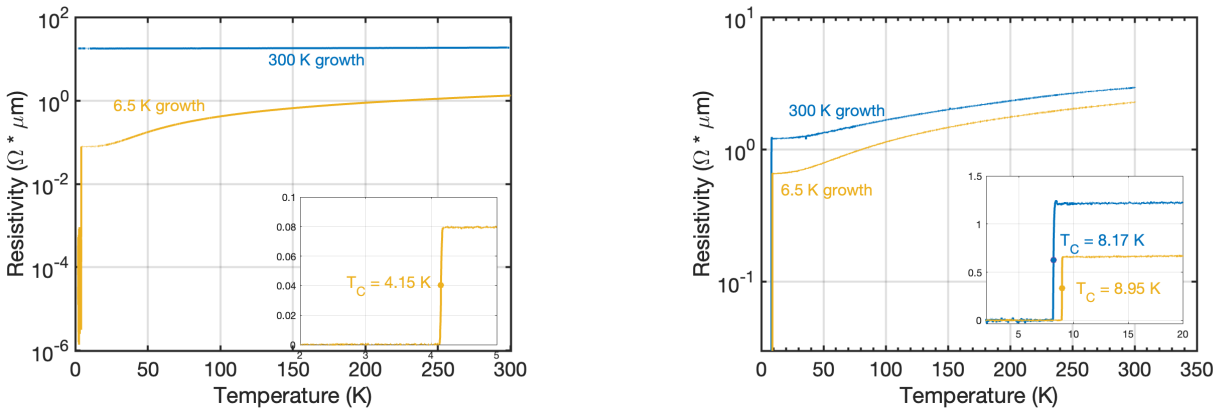

(a) (b)

FIG. 5: Resistivity vs. temperature for 50 nm a) Ta and b) Nb. The superconducting transition is represented as a dot where the resistivity is half the resistivity at 10 K.

RRR under LT growth. The T_C went from 8.17 K under RT growth to 8.95 K under LT growth. For RT and LT growth, we calculated a *RRR* of 2.44 and 3.48, respectively. Although these increases were not as significant as what was observed for Ta, this is still evidence that LT growth of Nb thin films result in higher T_C and *RRR* values, which is indicative of better film quality.

B. Critical Magnetic Field Comparison

Using the same method to calculate T_C, we calculated the H_C of our samples at different PPMS temperatures. Unlike T_C, H_C remained about the same when grown at LT as opposed to RT. Since RT grown Ta samples were not superconducting at or above 2 K, we omit the critical magnetic field comparison for Ta and focus solely on Nb. Figure 6 shows the critical magnetic field values for different constant PPMS temperatures. It was empirically determined that the relationship between H_C and temperature of the system is given by

$$H_C(T) = H_C(0)[1 - (T/T_{C_0})^2] \qquad (3)$$

where $H_C(0)$ is the critical magnetic field at zero temperature, T_{C_0} is the critical temperature in zero field, and T is the temperature of the system [12]. When plotting H_C against T, we use this relation as a fit.

The closeness of the fit curves in Figure 6 suggests that the critical magnetic fields remained about the same for LT and RT growth. However, in Figure 7, plotting resistivity against magnetic field for a constant temperature at 2 K, we saw

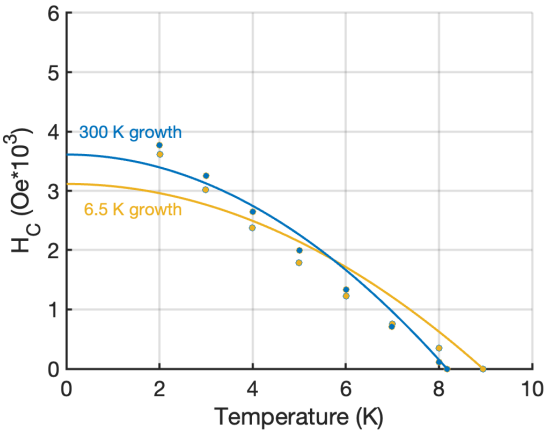

FIG. 6: Critical magnetic field versus temperature for 50 nm Nb.

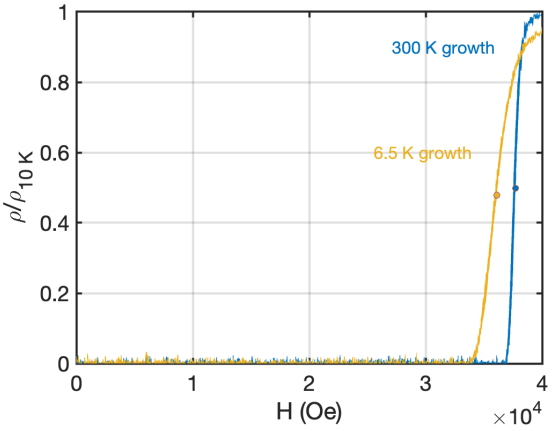

FIG. 7: Normalized resistivity vs. magnetic field for 50 nm Nb.

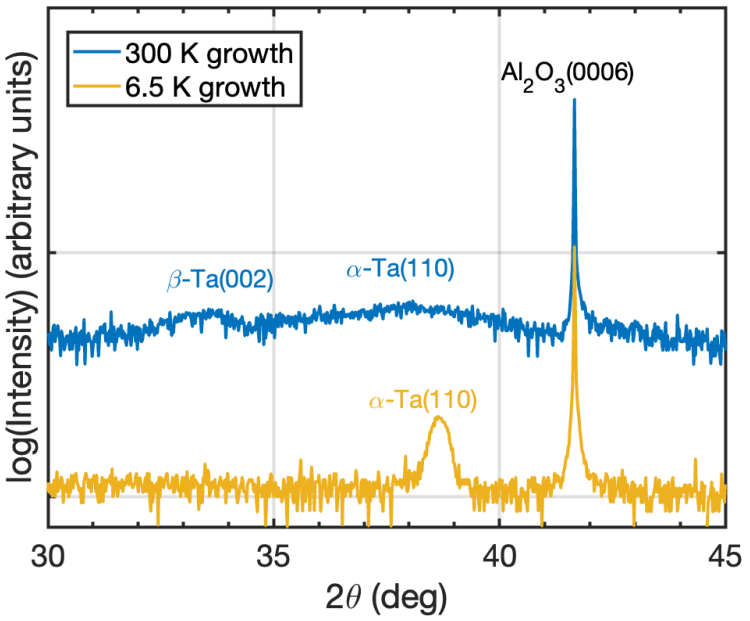

FIG. 8: XRD pattern for room temperature and low temperature grown 50 nm Ta thin films.

differences in the superconducting transition widths. Here, we use the resistivity of the sample at 10 K as a normalization factor. Under LT growth, the width increased for Nb. We speculate that this is due to structural differences between RT and LT grown films.

C. Structural Analysis: Atomic Force Microscopy and X-Ray Diffraction

We used AFM imaging to analyze the surface morphology of the RT and LT grown samples. To assess structural sample quality, we calculated the root mean square (RMS) roughness from the AFM images. The topography images for Ta show that LT growth resulted in smoother films with smaller grains. We calculated an RMS roughness of 1.565 nm and 0.447 nm for RT and LT grown Ta, respectively. However, for Nb, the AFM scans showed rougher films, with an increase in RMS roughness from 0.840 nm under RT growth to 1.228 nm under LT growth. This indicates a decrease in quality under LT growth for Nb thin films. We see that low temperature growth is not necessarily associated with smoother thin films, contrary to what we had predicted. We require scanning tunneling microscopy (STM) and transmission electron microscopy (TEM) imaging to look deeper into the surface morphology of the samples for better structural analysis.

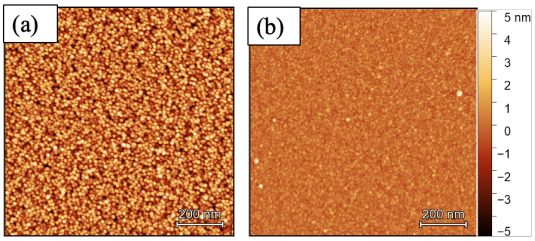

FIG. 9: AFM scans for 50 nm Ta under a) RT and b) LT growth.

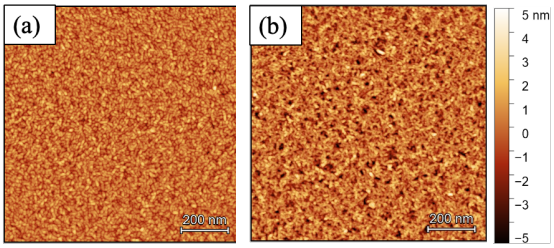

FIG. 10: AFM scans for 50 nm Nb under a) RT and b) LT growth.

To determine the crystal structure of the Ta films, we performed XRD spectroscopy and com-

pared room temperature and low temperature grown samples. Figure 8 shows the diffraction pattern obtained from the XRD measurements.

α-Ta peaks are expected at 38.5°, whereas β-Ta peaks are expected at 33.5°. It is clear from the XRD data that RT MBE produces a mix of the α and β phases of Ta, explaining why T_C was not observed above 2 K. For RT MBE, we see do not see peaks at the exact expected angle, suggesting low film quality. However, for LT MBE, we only see an α-Ta peak very close to 38.5°, indicating that we grow high quality α-Ta films. Our results show that the α-phase of Ta can also be stabilized by growing at low temperature, which results in T_C values expected for α-Ta.

D. Film Thickness Dependence

We investigated the effect of film thickness on the critical temperatures and magnetic fields of Ta and Nb samples. It is known that critical temperature is related to film thickness by

$$T_C(d) = T_{C_B} e^{-a/d} \tag{4}$$

where T_{C_B} is the critical temperature of the bulk, a is a constant depending on the bulk interaction potential and non-superconducting surface layer thickness, and d is the thickness of the superconducting film [13]. It is easy to see that as film thickness decreases, so does T_C, which affects film quality. Using ((4)) as a fit, we plotted the critical temperature as a function of thickness, and extracted the bulk temperature from the fit.

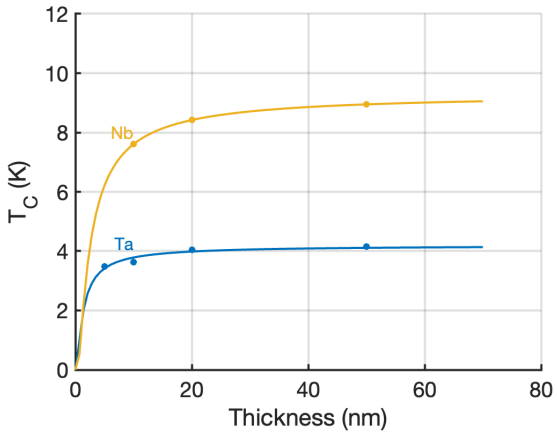

FIG. 11: Critical temperature versus thickness for LT grown Ta and Nb.

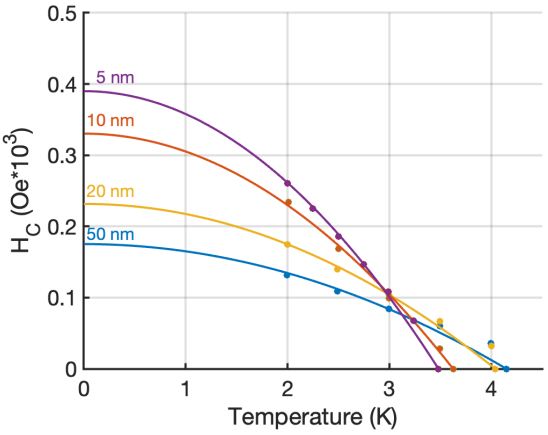

(a)

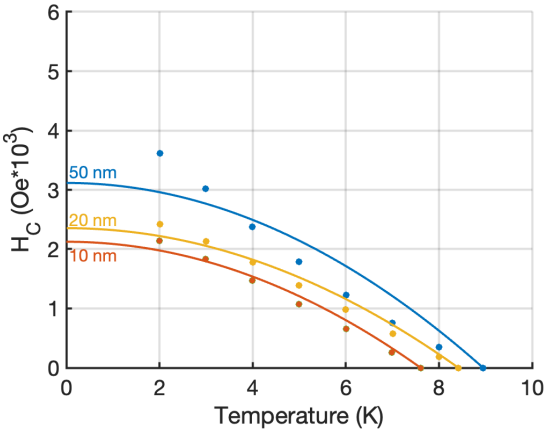

(b)

FIG. 12: Critical magnetic field vs. temperature at for different sample thicknesses for low temperature grown a) Ta and b) Nb.

As the sample thickness increases, the critical temperature approaches the bulk value. For LT grown Ta, we extracted a bulk T_C of 4.33 K. When grown at RT, bulk Ta has a T_C of less than 2 K. For LT grown Nb, we extracted a bulk T_C of 9.32 K. The known bulk critical temperature for RT grown Nb is between 9.25 K and 9.26 K, indicating that low temperature growth of Nb increases the critical temperature of the bulk [14]. From this data, we also see that using LT MBE, decreasing the film thickness still produces high critical temperature values that suggest good quality superconducting thin films.

We also analyzed the behavior of H_C under low temperature growth for different sample thicknesses. To do this, we constructed critical magnetic field versus temperature plots for Ta and Nb films of different thicknesses using 3 as a fit, shown in Figure

12. We calculated T_{C_0} using the method outlined in previous sections, and then we used (3) to fit our H_C vs. T data and extract $H_C(0)$. From this data for

Sample Thickness (nm)	T_{C_0} (K)	$H_C(0)(T)$
50	4.15	0.18
20	4.04	0.23
10	3.63	0.33
5	3.48	0.39

TABLE I: Low temperature grown tantalum dependence on thickness

Ta, we see that the T_{C_0} decreases with sample thickness, while $H_C(0)$ increases. Initially, we expected critical magnetic field to scale with critical temperature; that is, if critical temperature decreases with sample thickness, so should critical magnetic field. Although our results for Ta did not follow these expectations, our results for Nb did. These results sug-

Sample Thickness (nm)	T_{C_0} (K)	$H_C(0)(T)$
50	8.95	3.11
20	8.42	2.35
10	7.61	2.12

TABLE II: Low temperature grown Nb dependence on thickness

gest that critical magnetic fields do not necessarily scale with critical temperatures, as we had initially expected.

E. Substrate Dependence

To investigate the substrate dependence, we deposited 50 nm of each material on SiN_x, Si, and GaAs substrates. We compared the critical temperatures and critical magnetic fields of Ta thin films grown on these substrates. Figure 13 shows normalized resistivity plotted against temperature. Here, we observed critical temperatures of 4.15 K for on Al_2O_3, 4.13 K on SiN_x, 4.15 K on GaAs, and 4.21 K on Si. These results suggest that no matter the substrate, LT MBE growth of Ta thin films results in critical temperatures around 4.1 K. This is a promising result, compared to high temperature grown Ta thin films, which are typically limited to the use of sapphire or Si substrates [8]. This also suggests minimal reactions with the substrate during deposition.

We also compared the critical magnetic fields of Ta thin films grown on different substrates, shown in

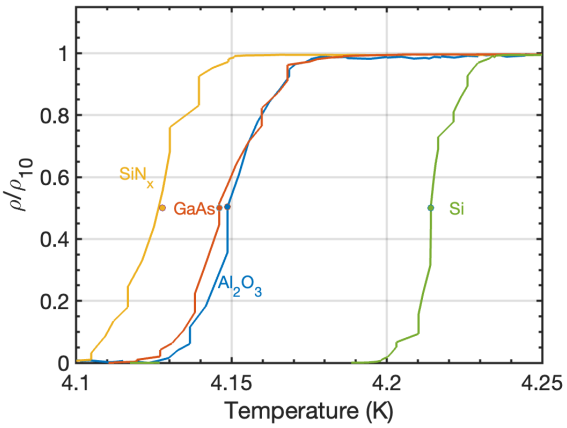

FIG. 13: Normalized resistivity versus temperature for LT grown Ta films on different substrates.

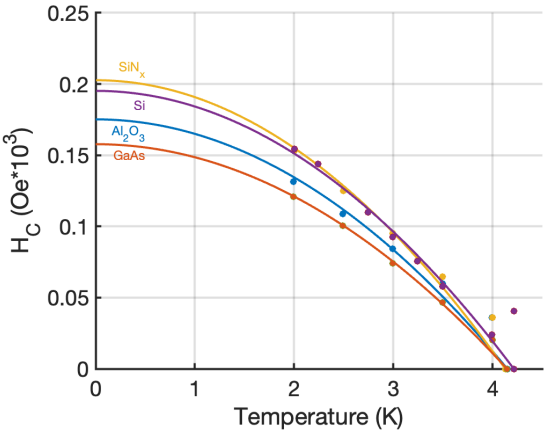

FIG. 14: Critical magnetic field versus temperature for temperature for grown Ta films on different substrates.

Figure 14. The closeness of the magnetic field curves indicates that the substrate does not change the critical magnetic field of Ta thin films when grown at LT.

Overall, we see that under LT growth, the use of different substrates does not significantly affect the superconducting properties of Ta thin films. This indicates a lack of epitaxy between the substrate and superconducting material at the interface, compared to high temperature growth.

IV. CONCLUSIONS

In this work, we investigated how low temperature molecular beam epitaxy growth affects the critical temperatures, critical magnetic fields, and struc-

ture of Ta and Nb thin films on sapphire substrates, compared to room temperature growth. Our results show that LT MBE produces superconducting Ta and Nb thin films with higher critical temperatures, which is an indication of higher electrical quality. We also a see different crystal structure in the Ta films, since LT MBE produces the α phase of Ta, whereas RT MBE produces the mixed phase. These structural and electrical differences suggest that LTMBE growth could produce superconductors better suited for qubit systems. However, despite the improvement in electrical quality for Nb thin films, we observe a decrease in film quality for Nb from the AFM images, motivating other methods of microscopy and structural analysis. We also found that reducing the thickness of Ta and Nb thin films also results in comparably high critical temperature values, which will be useful in the field of topological quantum computing, allowing us to achieve practically two-dimensional superconducting films. Finally, we were able to achieve high critical temperature values when growing Ta thin films on SiN_x, GaAs, and Si substrates at low temperature. These results might suggest that LT MBE growth reduces the amount of interaction at the superconductor-substrate interface, leading to better structural quality of the thin films, compared to high temperature growth. With these findings, Ta and Nb thin film superconductors can be used in all sorts of devices that might require different substrates. Low temperature molecular beam epitaxy presents as a promising technique for growing higher quality superconducting thin films for Ta and Nb, and potentially other superconductors such as vanadium and aluminum. Such improvements in superconductor quality can also improve coherence times when implemented in qubits, and our results may boost the practicality of quantum computing in the future.

V. ACKNOWLEDGEMENTS

I am very grateful for Professor Christopher Palmstrøm's guidance and support throughout the REU program – his enthusiasm and warmth played a huge role in the success of this project. I also thank him for giving me the experience of working in a lab with such incredible facilities and learning opportunities. Additionally, I owe much of the success to my graduate advisor Teun van Schijndel, without whom I would not have learned so much about molecular beam epitaxy and superconductivity. Finally, I must thank the REU site director Professor Sathya Guruswamy, who accepted me into this wonderful program and wholeheartedly supported my pursuit of condensed matter physics. This work was funded by the National Science Foundation, Grant PHY-1852574.

[1] P. Krantz, M. Kjaergaard, F. Yan, T. P. Orlando, S. Gustavsson, and W. D. Oliver, Appl. Phys. Rev. 10.1063/1.5089550 (2019).

[2] M. H. Devoret and J. M. Martinis, Quantum Information Processing **3**, 10.1007/s11128-004-3101-5 (2004).

[3] C. Wang, X. Li, H. Xu, Z. Li, J. Wang, Z. Yang, Z. Mi, X. Liang, T. Su, C. Yang, G. Wang, W. Wang, Y. Li, M. Chen, C. Li, K. Linghu, J. Han, Y. Zhang, Y. Feng, Y. Song, T. Ma, J. Zhang, R. Wang, P. Zhao, W. Liu, G. Xue, Y. Jin, and H. Yu, npj Quantum Information **91**, 10.1038/s41534-021-00510-2 (2022).

[4] V. T. Lahtinen and J. K. Pachos, SciPost Phys. **3**, 10.21468/SciPostPhys.3.3.021 (2017).

[5] V. Mourik, K. Zuo, S. M. Frolov, S. R. Plissard, E. P. A. M. Bakkers, and L. P. Kouwenhoven, Science **336**, 10.1126/science.1222360 (2012).

[6] J. Yu, J. Yu, Y. Zhao, R. Pan, X. Zhou, and Z. Wei, ACS Omega **8**, doi.org/10.1021/acsomega.2c06324 (2023).

[7] A. P. M. Place, L. V. H. Rodgers, P. Mundada, B. M. Smitham, M. Fitzpatrick, Z. Leng, A. Premkumar, J. Bryon, A. Vrajitoarea, S. Sussman, G. Cheng, T. Madhavan, H. K. Babla, X. H. Le, Y. Gang, B. Jäck, A. Gyenis, N. Yao, R. J. Cava, N. P. de Leon, and A. A. Houck, Nature Communications **12**, 10.1038/s41467-021-22030-5 (2021).

[8] Y. Urade, K. Yakushiji, M. Tsujimoto, T. Yamada, K. Makise, W. Mizubayashi, and K. Inomata1, arXiv:2306.15258v1 [quant-ph] 10.48550/arXiv.2306.15258 (2023).

[9] C. R. H. McRae, H. Wang, J. Gao, M. Vissers, T. Brecht, A. Dunsworth, D. Pappas, and J. Mutus, Rev. Sci. Instrum. **91**, 10.1063/5.0017378 (2020).

[10] A. J. Ferguson, N. A. Court, F. E. Hudson, and R. G. Clark, in *2006 International Conference on Nanoscience and Nanotechnology* (2006).

[11] A. Premkumar, C. Weiland, S. Hwang, B. Jäck, A. P. M. Place, I. Waluyo, A. Hunt, V. Bisogni, J. Pelliciari, A. Barbour, M. S. Miller, P. Russo, F. Camino, K. Kisslinger, X. Tong, M. S. Hybertsen, A. A. Houck, and I. Jarrige, Communications Materials **2**, 10.1038/s43246-021-00174-7 (2021).

[12] M. Tinkham, *Introduction to Superconductivity*, 2nd ed. (Courier Corporation, Mineola, New York, 1973).

[13] M. S. M. Minhaj, S. Meepagala, J. T. Chen, and L. E. Wenger, Phys. Rev. B **49**, 10.1103/PhysRevB.49.15235 (1994).

[14] T. Nishizaki1, K. Edalati, S. Lee4, Z. Horita, T. Akunel, T. Nojima, S. Iguchi, and T. Sasaki5, Materials Transactions **60**, 10.2320/matertrans.MF201940 (2019).